npg

Matrix metalloproteinase-9 mediates hypoxia-induced vascular leakage in the brain via tight junction rearrangement

Alexander T Bauer, Heinrich F Bürgers, Tamer Rabie and Hugo H Marti

Institute of Physiology and Pathophysiology, University of Heidelberg, Heidelberg, Germany

Blood–brain barrier (BBB) disruption, resulting from loss of tight junctions (TJ) and activation of matrix metalloproteinases (MMPs), is associated with edema formation in ischemic stroke. Cerebral edema develops in a phasic manner and consists of both vasogenic and cytotoxic components. Although it is contingent on several independent mechanisms, involving hypoxic and inflammatory responses, the single effect of prolonged hypoxia on BBB integrity *in vivo* was not addressed so far. Exposing mice to normobaric hypoxia (8% oxygen for 48 h) led to a significant increase in vascular permeability associated with diminished expression of the TJ protein occludin. Immunofluorescence studies revealed that hypoxia resulted in disrupted continuity of occludin and zonula occludens-1 (Zo-1) staining with significant gap formation. Hypoxia increased gelatinolytic activity specifically in vascular structures and gel zymography identified MMP-9 as enzymatic source. Treatment with an MMP inhibitor reduced vascular leakage and attenuated disorganization of TJ. Inhibition of vascular endothelial growth factor (VEGF) attenuated vascular leakage and MMP-9 activation induced by hypoxia. In conclusion, our data suggest that hypoxia-induced edema formation is mediated by MMP-9-dependent TJ rearrangement by a mechanism involving VEGF. Therefore, inhibition of MMP-9 might provide the basis for therapeutic strategies to treat brain edema.

Introduction

The blood–brain barrier (BBB) is a physical and metabolic barrier that separates the peripheral circulation from the central nervous system and serves to regulate and protect the microenvironment of the brain. Central nervous system injuries, such as ischemia and hypoxia, lead to changes of the BBB integrity and cause edema formation (Hackett and Roach, 2001; Sandoval and Witt, 2008). Low BBB permeability is maintained by brain microvascular endothelial cells (BMECs) through tight junctions (TJ), and the basal lamina, containing extracellular matrix proteins (Hawkins and Davis, 2005). The BMECs act in concert with adjacent astrocytes, pericytes, neurons, and the extracellular matrix to restrict the entry of potentially damaging blood-borne substances into the brain parenchyma (Sandoval and Witt, 2008).

The TJ of the BBB are composed of a combination of transmembrane and cytoplasmatic proteins. The transmembrane proteins critical for paracellular function at BBB are occludin and claudins (Hawkins and Davis, 2005). Claudins are small transmembrane proteins (20 to 24 kDa) that span the membrane four times, of which claudin-1, -3, and -5 were shown to be expressed in endothelial cells of the BBB. Occludin is a 60-kDa integral membrane protein with four transmembrane segments. Zonula occludens-1 (Zo-1) is the primary cytoplasmatic protein associated with TJ. It links the C-terminal ends of occludin and claudins to the underlying actin cytoskeleton (Hawkins and Davis, 2005).

Matrix metalloproteinases (MMPs) are zinc-dependent endopeptidases, secreted as zymogens, which must be cleaved to be fully active. The MMPs are classically known as matrix-degrading enzymes involved in many physiologic processes (Rosenberg, 2009), but they are also implicated in BBB opening as part of the neuroinflammatory response in ischemia, multiple sclerosis, and infection (Cunningham *et al*, 2005). Dysregulation of MMPs may be involved in

838

brain damage by digesting matrix substrates and interrupting cell–cell or cell–matrix interactions necessary for cell survival (Rosenberg, 2009). In particular, MMP-2 and MMP-9, also known as gelatinase A and gelatinase B or type IV collagenases, are upregulated in cerebral ischemia and closely associated with BBB disruption (Yang et al, 2007) and edema formation (Gasche et al, 2001). In addition, accumulating evidence indicates that stroke increases BBB permeability, mediated via TJ disruptions with an involvement of MMPs (Yang et al, 2007). Vasogenic edema formation occurs in a phasic manner that involves a complex network of independent mechanisms, such as angiogenesis, inflammatory processes, and oxidative stress (Hawkins and Davis, 2005; Sandoval and Witt, 2008). Thus, although several factors have been identified in the regulation of BBB permeability during inflammatory processes and ischemia in vivo, the underlying molecular and pathogenic mechanisms of vascular leakage by exposure to hypoxia in vivo are poorly understood. This is of clinical relevance during hypoxic exposure at high altitudes, as high altitude cerebral edema formation has not only a cytotoxic but also a vasogenic component (Kallenberg et al, 2007). A number of studies using in vitro and in situ BBB models have shown that during hypoxia, the localization of TJ proteins is disrupted (Fischer et al, 2000; Mark and Davis, 2002). Furthermore, we previously showed that hypoxia-induced hyperpermeability in the brain is dependent on vascular endothelial growth factor (VEGF) expression, as inhibition of VEGF activity using a neutralizing antibody completely blocked hypoxia-induced leakage of the BBB in vivo (Schoch et al, 2002).

In an attempt to further characterize the mechanisms underlying hypoxia-induced vascular leakage in vivo, we quantified hypoxia-induced permeability changes, and examined protein expression and cellular localization of occludin, claudin-5, and Zo-1 in mouse brain in vivo during normobaric hypoxia. To investigate the role of MMP activation for hypoxia-induced edema formation in vivo, we performed both in situ as well as gel zymography to localize and quantify MMP activity. Furthermore, the potency of a specific MMP inhibitor to counteract vascular leakage and TJ rearrangement in vivo was tested. Finally, the effect of VEGF inhibition on vascular leakage and MMP activation was analyzed.

Materials and methods

Hypoxic Exposure

All experiments were performed with male NMRI mice (20 to 30 g) and were approved by the governmental animal care authorities (35-9185. 81/G-97/04). Mice were exposed to normobaric hypoxia at 8% oxygen for 48 h or were kept at room air as described (Schoch et al, 2002). Thereafter, mice destined for histologic and biochemical analysis were killed by decapitation, brains were removed and snap frozen at

$-80°C$ or embedded in Tissue Tek for cryosectioning. The broad-spectrum MMP inhibitor, p-aminobenzoyl-gly-pro-D-leu-D-ala-hydroxamate (AHA; Sigma, Steinheim, Germany; MW: 491), that has previously been used to inhibit MMP activity in the brain in vivo (Gasche et al, 2001; Rosenberg, 2009) was dissolved in phosphate-buffered saline (PBS) and injected (60 mg/kg) ip (intraperitoneal) (18 mice) before normoxic or hypoxic exposure (Gasche et al, 2001). The same amount of PBS was given as control (18 mice). In another set of experiments, bevacizumab (Avastin, Roche, Mannheim, Germany) was delivered ip at 10 mg/kg in saline immediately before hypoxic or normoxic exposure (24 mice). Control mice (24 animals) were treated with an equal volume of saline.

Quantification of Vascular Permeability In Vivo

Vascular permeability was assessed in 68 mice with sodium fluorescein as described (Schoch et al, 2002), except that perfusion through the left heart ventricle was performed with 10 mL PBS (120 mL/h) using an infusion pump (PP50; Asid Bonz, Herrenberg, Germany). Fluorescence of supernatant was measured at 485 nm with an excitation wavelength of 528 nm using a fluoroscope (Synergy HT; Bio-Tek, Bad Friedrichshall, Germany). Results are presented as relative fluorescence units (r.f.u.) per mg of brain tissue.

Western Blot Analysis

Both brain hemispheres of hypoxic mice and controls (30 animals) were homogenized in 1 mL of lysis buffer (0.5% Nonidet P-40, 1% Triton-X-100, 20 mmol/L Tris (pH = 7.6), 250 mmol/L NaCl, 1 mmol/L DTT, 1 mmol/L EDTA, 1 mmol/L EGTA, 1 mmol/L PMSF, 1% Protease Inhibitor Cocktail (Sigma)) and centrifuged. Supernatants were used for SDS-PAGE. Protein was quantified using Bradford assay (Biorad, München, Germany) with bovine serum albumin (BSA) as standard. After SDS-PAGE, proteins were transferred onto PVDF (Millipore, Schwallbach, Germany) or nitrocellulose (Whatman, Dassel, Germany) membranes. Membranes were blocked for 1 h in 5% (w/v) BSA in TBS-T buffer (Tris-buffered saline with 0.1% Tween 20) and immersed for at least 2 h at room temperature with antibodies against claudin-5 (35-2500; Zymed, Invitrogen, Karlsruhe, Germany), occludin (71-1500; Zymed), or Zo-1 (61-7300; Zymed), each diluted 1:250 to 1:500 in blocking solution, followed by washing and incubation with peroxidase-conjugated goat-anti-rabbit antibody (Zymed), diluted 1:5000 in 5% BSA/TBS-T for 1 h at room temperature, again washed, and finally visualized as described before (Kilic et al, 2006). Blot images were scanned, protein levels analyzed densitometrically with Image J software, corrected for protein load determined by actin staining (A 2006; Sigma), and expressed as relative values compared with normoxic controls.

Immunofluorescence

Brain cryosections (10 μm) from 20 mice were fixed in ice-cold acetone for 2 mins, washed and blocked for 30 mins in 10% (v/v) goat serum dissolved in 0.1 M PBS containing 0.1% Tween 20 (PBS-T) and incubated for 4 h at room

temperature with following primary antibodies: anti-claudin-5, anti-occludin, and anti-Zo-1, diluted 1:100 in PBS-T. After washing, sections were incubated for 1 h with secondary Cy3-conjugated IgG goat anti-rabbit or Cy2-conjugated IgG goat anti-mouse antibodies (Jackson ImmunoResearch, Hamburg, Germany) diluted 1:500 in blocking solution. Co-staining was performed overnight at 4°C with rat anti-platelet endothelial cell adhesion molecule-1 (Pecam-1; 557355, BD Biosciences, Heidelberg, Germany) 1:60 in PBS-T, followed by Cy2-conjugated IgG goat anti-rat antibody or Cy3-conjugated IgG rabbit anti-rat (1:500; Jackson Immuno-Research). Nuclei were stained with 4,6-diamidino-2-phenyl-indole (DAPI) (1:5000 in PBS) for 10 mins. Sections were embedded with Mowiol and viewed with a fluorescent microscope (BX50; Olympus, Hamburg, Germany). Confocal microscopy was acquired using a confocal laser-scanning microscope (Eclipse 80i; Nikon, Düsseldorf, Germany) under a $60 \times$ oil-immersion objective and data were analyzed by Image J. Gap length is presented as percentage (%) of whole TJ staining of occludin, and Zo-1, respectively. At least six vessels per brain were analyzed.

In Situ Zymography

In situ gelatinolytic activity was assessed using a commercially available kit (Molecular Probes, Karlsruhe, Germany). Cryosections (10 µm) were incubated for 3 to 6 h at 37°C in a humidified chamber in a reaction buffer containing the gelatin fluorescein conjugate (50 µg/mL) without washing. Identification of vessels was performed by immunofluorescence co-staining with anti-Pecam-1, followed by Cy3-conjugated IgG rabbit anti-rat antibodies. Nuclei were stained with DAPI (1:5000 in PBS) for 10 mins. Sections were embedded with Mowiol and examined microscopically at the same anatomic levels (Axiovert200M, Zeiss, Jena, Germany; BX50, Olympus). Data were analyzed with Image J and TissueQuest software.

Gelatin Gel Zymography

Gel zymography was performed as described (Kleiner and Stetler-Stevenson, 1994) with some modifications. Brain hemispheres from hypoxic or control mice (20 animals) were homogenized with lysis buffer (50 mmol/L Tris/HCl pH 7.5, 75 mmol/L NaCl, 1 mmol/L PMSF, and 0.5% Triton X-100). After incubation for 1 h at 4°C with 400 r.p.m. and centrifugation (20 mins, 10,000 r.p.m., 4°C), supernatants were incubated with 50% $(NH_4)_2SO_4$ for 15 mins for extraction of MMP-2 and MMP-9 and centrifuged. Pellets were resuspended in 250 µL 50 mmol/L Tris/HCl, pH = 7.5 and incubated with 100 µL Gelatine-Sepharose 4B beads (Amersham, GE healthcare, München, Germany) for 2 h at 4°C with gentle shaking. Beads were collected, and the MMPs eluted by incubation with 200 µL of elution buffer (50 mmol/L Tris/HCl, 1 M NaCl, 10 mmol/L CaCl_2, 7.5% DMSO) for 1 h at 4°C with gentle shaking. Equal amounts of samples were electrophoretically separated on 7.5% SDS-PAGE gels co-polymerized with 2 mg/mL gelatin (Sigma) under nonreducing conditions.

Gels were incubated in washing buffer containing 2.5% Triton X-100 and then incubated for 40 h in developing buffer (50 mmol/L Tris/HCl, 10 mmol/L CaCl_2, 0.02% NaN_3)

at 37°C before staining with Coomassie blue R-250 (250 mL Methanol, 35 mL acetic acid, 1.25 g Brilliant Blue) for 1 h. Gels were destained in 5% acetic acid and 25% methanol until clear bands manifesting gelatinolysis appeared on the blue background. Mixed human MMP-2 and MMP-9 standards (CC073; Chemicon, Hofheim, Germany) were used as positive control. Relative gelatinolytic activity was quantified via measurement of optical density using Image J and expressed as the ratio of loaded normoxic controls.

Statistical Analysis

For statistical analyses, the unpaired Student's *t*-test was used. Values were expressed as the mean ± s.d. Results were considered as statistically different at $P < 0.05$.

Results

Hypoxia Induces Vascular Leakage *In Vivo*

To mimic the oxygen partial pressure at 7500 m altitude, we exposed mice to 8% oxygen for 48 h. Using sodium fluorescein as tracer, we found that hypoxia increased relative fluorescence intensity in brain lysates 1.8-fold ($P < 0.05$) compared with normoxic controls, indicating an increased permeability in cerebral microvasculature. Fluorescence in control brains ($n = 11$ animals) was 10.30 ± 3.12 r.f.u./mg brain tissue and increased to 18.20 ± 4.18 r.f.u./mg brain tissue ($n = 15$ animals) after 48 h exposure to 8% oxygen (data not shown).

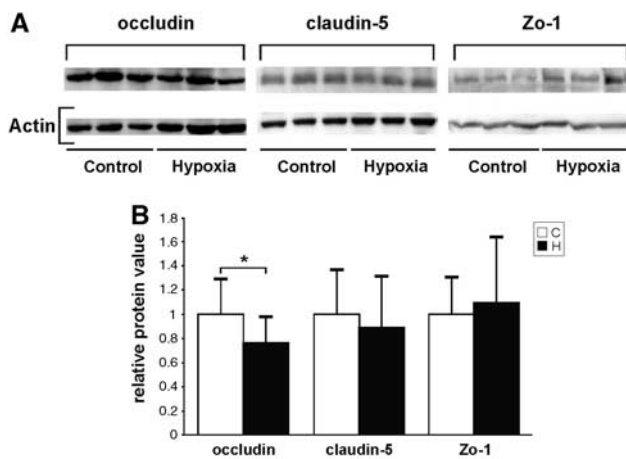### Hypoxia Reduces Occludin Expression

To determine whether hypoxia-induced hyperpermeability was due to TJ alterations, expression of the TJ-associated proteins occludin, claudin-5, and Zo-1 was quantified in brain lysates by western blot analysis (Figure 1). The antibodies against occludin, Zo-1, and claudin-5 recognized bands at the expected molecular weights of about 60, 220, and 22 kDa (Figure 1A). Hypoxia resulted in a significant reduction by 20% of occludin expression (Figure 1B), whereas no change in the expression levels of Zo-1 and claudin-5 was found.

Rearrangement and Gap Formation of Occludin and Zonula Occludens-1 after Hypoxic Exposure

To further investigate alterations of TJ protein expression *in situ*, localization of claudin-5, occludin, and Zo-1 was analyzed in cerebral vascular structures, identified by co-staining with Pecam-1. Claudin-5 showed a staining along the margins of cell–cell contacts and diffuse punctate distribution in the cytoplasm. Little change of the localization pattern of claudin-5 was observed during hypoxia (Figure 2A). Staining of occludin and Zo-1 was continuously and sharply located on the endothelial cell margin of cerebral microvessels in normoxic controls (Figure 2A,

840

arrows). By contrast, occludin and Zo-1 showed a typical rearrangement with diffuse and discontinuous staining and significant disruptions after hypoxic exposure (Figure 2A, arrowheads).

Confocal microscopy analysis and three-dimensional reconstruction of vascular structures revealed that occludin and Zo-1 showed predominant expression along the margin of cell–cell contacts, as shown in immunofluorescence experiments before. Whereas normoxic vessels showed a linear, regular labeling of occludin and Zo-1 (Figures 2B and 2D, arrows), hypoxia induced a discontinuous staining of the TJ proteins with gap formation (Figures 2B and 2D, arrowheads). Quantitative analysis revealed a total gap length for occludin of $1.1\% \pm 0.68\%$ in normoxic control vessels, which increased to $7.8\% \pm 3.6\%$ after hypoxic exposure (Figure 2C), and $1.54\% \pm 1.33\%$ disruption in normoxic control versus $6.8\% \pm 3.3\%$ in hypoxic vessels for Zo-1 (Figure 2E). Thus, in vivo hypoxia is associated with gap formation and rearrangement of the TJ proteins occludin and Zo-1, but not claudin-5.

Figure 1 Western blots showing reduction of occludin expression after hypoxic exposure. Total protein was extracted from the brains of control (C) mice and mice exposed to 8% oxygen for 48 h (H). (**A**) Western blots showing reduced occludin expression in hypoxia, but little effect on claudin-5 and Zo-1 expression. Representative samples of three animals in both groups are shown. (**B**) Quantification and normalization to actin showed significant reduction of occludin expression and little change of claudin-5 and Zo-1 in hypoxia. Values are mean ± s.d. (*$P < 0.05$; $n = 7$ to 14 animals).

Hypoxia Induces Matrix Metalloproteinase Activation in Cerebral Microvasculature

In an attempt to characterize the underlying mechanisms of TJ gap formation and rearrangement, in situ zymography was used to assess the presence and regulation of gelatinase activity. To identify the endothelial cell origin of proteolytic activity, we performed immunofluorescence co-staining with Pecam-1. Although gelatinase activity was hardly detectable in normoxic vessels (Figure 3A, arrowheads) a clearly increased gelatinolytic activity was seen in hypoxic vessels (Figure 3A, arrows), whereas nonvascular gelatinase activity remained unchanged, suggesting that during hypoxia gelatinase activity is primarily increased in vascular structures. Quantification revealed that hypoxic exposure resulted in a two- to four-fold increase in all brain areas in the number of microvessels positive for gelatin degradation, especially in cerebral cortex, thalamus, and hypothalamus (Figure 3B).

Gelatinase activity found in hypoxic vessels is thought to result from increased MMP activation. As in situ zymography cannot distinguish between MMP-2 and -9, and appropriate antibodies were not available for mouse tissue, we performed gelatin-substrate gel zymography and assessed MMP gelatinase activity in whole tissue extracts of brain hemispheres to identify the source of gelatinase activity. Latent proMMP-9 and proMMP-2 were detected both in control and hypoxic brains (Figure 4A). After hypoxic exposure, proMMP-9 activity significantly increased in hypoxic brains when compared with normoxic controls (Figures 4A and 4B). Furthermore, a second band corresponding to the activated form of MMP-9 appeared after hypoxia (Figures 4A and 4C). Unlike MMP-9, no difference in proMMP-2 activity and no activated MMP-2 were detected in hypoxic brains, suggesting that during brain hypoxia MMP-9, but not MMP-2 is preferentially activated (Figures 4A–4C).

Matrix Metalloproteinase-9 Inhibition Reduces Hypoxia-Induced Hyperpermeability and Gap Formation

To establish whether MMP activation is responsible for hypoxia-induced vascular leakage and TJ rearrangement, animals were treated with the MMP

Figure 2 Hypoxia correlates with localization changes of occludin and Zo-1. Mice were exposed for 48 h to 20% (control) or 8% oxygen (hypoxia). At least six coronal brain sections per animal were stained for claudin-5, occludin, or Zo-1 and co-stained with platelet endothelial cell adhesion molecule-1 (Pecam-1). Nuclei were stained with 4,6-diamidino-2-phenylindole (DAPI). Representative pictures for both groups are shown. (**A**) Vessels in the cortex of control mice showed a continuous, linear labeling of occludin and Zo-1 along the whole vessel (arrows). In hypoxic brains, a discontinuous, less regular distribution of Zo-1 and occludin in the vessels was noted (arrowheads) ($n = 6$ animals). Little change was seen in the distribution pattern of claudin-5. (**B**, **D**) Three-dimensional reconstruction after confocal microscopy demonstrates localization changes of occludin and Zo-1. The TJ proteins (green) are located at the cell margins (arrows) of Pecam-1-positive endothelial cells (red). Hypoxic vessels showed an irregular and diffuse staining and gap formation (arrowheads). (**C**, **E**) To quantify disruption and gap formation, gap length was measured (in % of complete staining). Hypoxia significantly increased gap length and disruption of occludin and Zo-1. Values are mean ± s.d. (*$P < 0.001$; $n = 5$ animals).

inhibitor AHA. During hypoxia, AHA completely blocked gelatin degradation by MMP-9, but had no effect on MMP-2 activity (Figures 4A–4C). With AHA treatment, proMMP-9 activity during hypoxia was even significantly lower compared with basal activity in normoxic controls (Figure 4B).
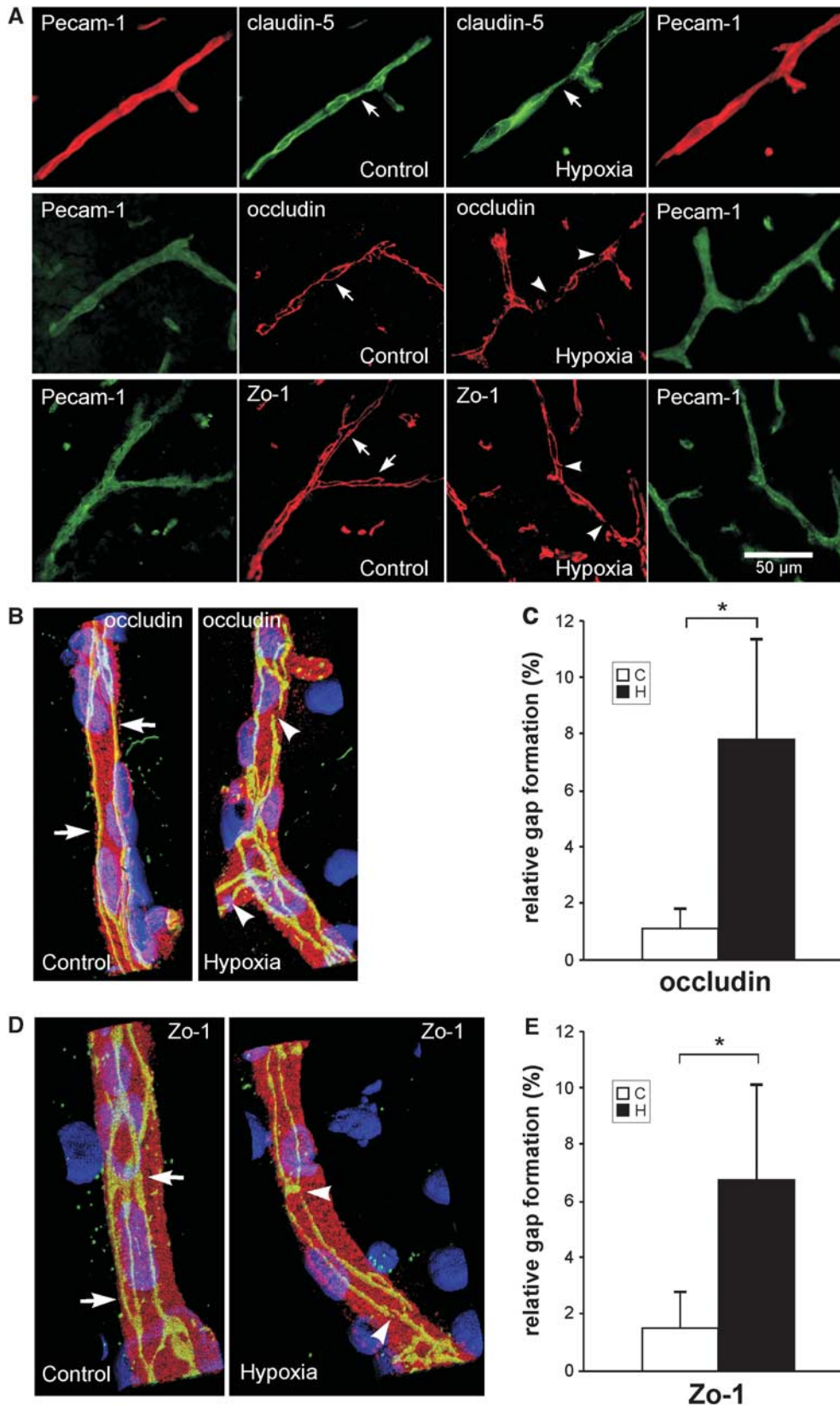
Pretreatment with AHA significantly attenuated the hypoxic increase in permeability from 29.99 ± 8.01 r.f.u./mg brain tissue $(n = 5)$ after hypoxia (H) to 21.97 ± 2.47 $(n = 5)$. The normoxic controls showed 14.04 ± 5.77 r.f.u./mg brain tissue $(n = 4)$ (C), Thus, AHA reduced hypoxic permeability by almost 30% (Figure 5), whereas it had no effect in normoxic control mice (16.94 ± 2.86 r.f.u./mg brain tissue, $(n = 4)$).
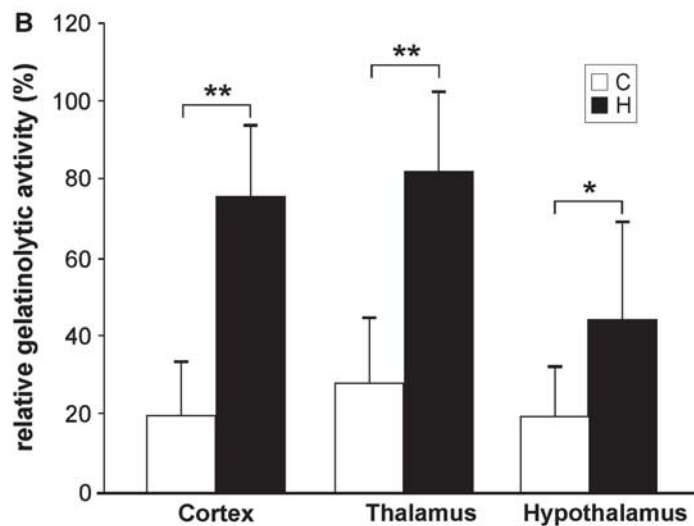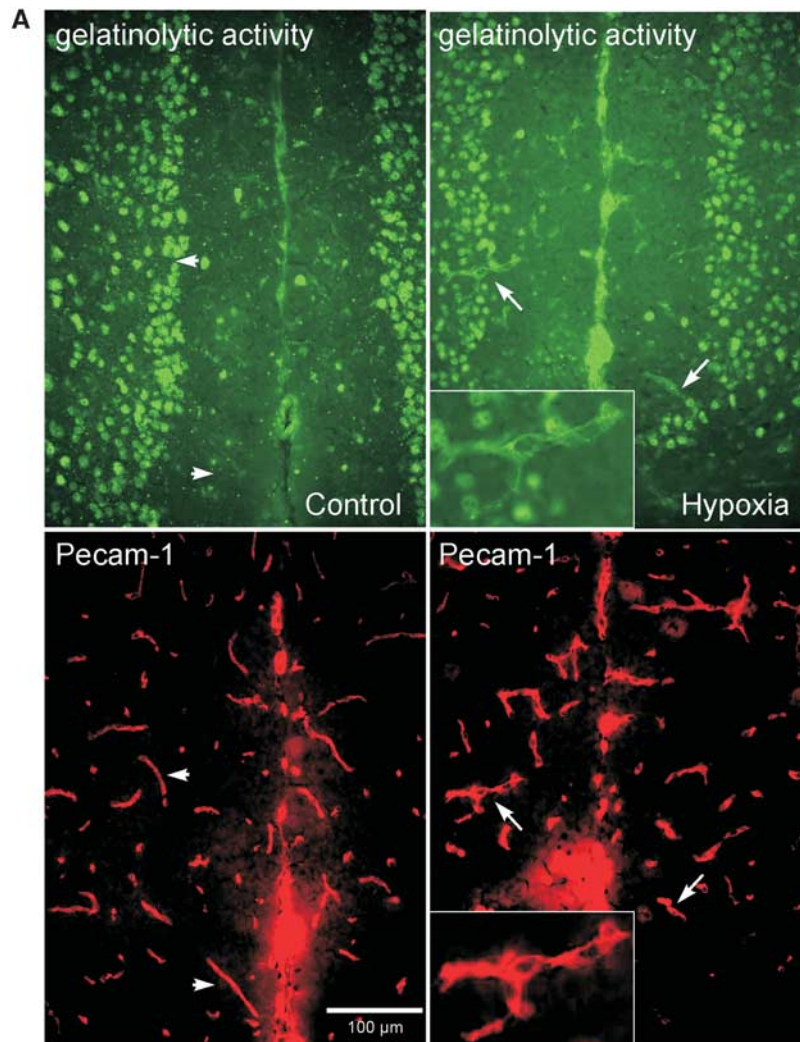
We next examined whether MMP inhibition can revert hypoxia-induced changes of TJ distribution. Presence of AHA clearly reduced disruption of occludin and Zo-1 staining (Figures 6A and 6C). Hypoxia-induced gap formation of occludin decreased from 7.8% ± 3.6% to 5.2% ± 2.4% (Figure 6B) and Zo-1 gaps from 6.8% ± 3.3% to 2.5% ± 1.4% (Figure 6D).

Taken together, the MMP inhibitor AHA significantly reduced hypoxia-induced permeability and TJ gap formation, implicating vascular MMP activation in hypoxia-induced TJ changes and edema formation in the brain.

Vascular Endothelial Growth Factor Inhibition Attenuates Vascular Leakage and Matrix Metalloproteinase-9 Activation During Hypoxia

To study the molecular mechanisms of MMP-9 activation in hypoxia-induced vascular permeability, we examined possible interactions between VEGF and the MMP system. Treatment with the anti-VEGF antibody bevacizumab (Avastin) significantly reduced hypoxic vascular leakage as expected (Schoch et al, 2002) (from 22.99 ± 6.52 r.f.u./mg (H) to 16.22 ± 3.61 r.f.u./mg (H + αVEGF), but had no effect in normoxic controls (11.91 ± 3.37 r.f.u./mg (C + αVEGF) versus 10.56 ± 1.83 r.f.u./mg (C) ($n = 6$ animals per group) (Figure 7A).

To determine whether VEGF inhibition also reduced activity of MMP-9, gelatinolytic activity was measured by gel zymography ($n = 3$ to 6 animals per group) (Figure 7B). Treatment with bevacizumab significantly attenuated MMP-9 activity during hypoxia (Figure 7B), suggesting that hypoxia-induced MMP-9 activation is dependent on VEGF stimulation. No significant effect on MMP-2 activity was found (Figure 7B).

Discussion

The main findings of this study are that (1) hypoxia-induced vascular leakage in vivo is the result of gap formation and rearrangement of TJ proteins, (2)
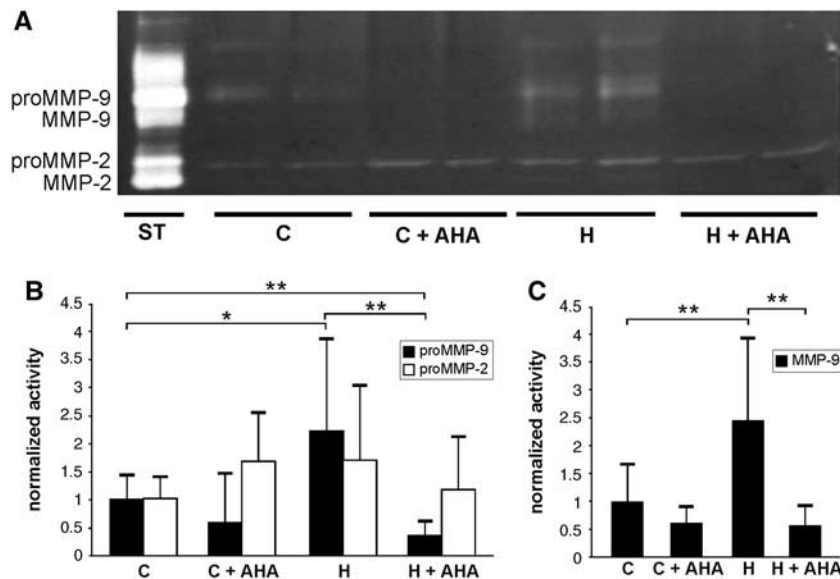
Figure 4 Hypoxia upregulates cerebral MMP-9. (**A**) Representative gelatin zymography demonstrating upregulation of the proform of MMP-9 (proMMP-9) activity after 48 h of hypoxia (H), compared with normoxic control (C). A second band corresponding to the cleaved-activated MMP-9 enzyme was detected in hypoxia only. Using the specific MMP inhibitor p-aminobenzoyl-gly-pro-D-leu-D-ala-hydroxamate (AHA), proMMP- and MMP-9 upregulation in hypoxia was completely blocked. ProMMP-2 activity was unchanged and no activated MMP-2 was detected in hypoxia. ST: standards as positive controls for MMP-2 and MMP-9. (**B**) Densitometric quantification showing significantly increased proMMP-9 in hypoxia, and no change for proMMP-2. The MMP inhibition strongly reduced hypoxia-induced activity of proMMP-9, even below the normoxic activity level, but had no effect on pro-MMP-2 (**C**) Elevated activation of MMP-9 in hypoxia was completely blocked by AHA. Bars show mean values (± s.d.) of relative gelatinolytic activity (*$P < 0.05$, **$P < 0.005$; $n = 3$ to 6 animals per group).

Figure 3 In situ zymography shows increased gelatinolytic activity in brain microvasculature after hypoxic exposure. Cryosections were incubated with gelatin-FITC substrate for 3 h and vascular structures were co-stained with platelet endothelial cell adhesion molecule-1 (Pecam-1; red). (**A**) Representative pictures showing no gelatinolytic activity (green) in normoxic control vessels (arrowheads) but clearly increased activity in hypoxia (arrows). Inlays show higher magnification of a labeled vascular structure. (**B**) Quantification revealed a two- to four-fold increase in the number of microvessels showing gelatinolytic activity in cortex, thalamus, and hypothalamus (*$P < 0.0001$, **$P < 0.000001$; $n = 5$ animals per group).

844
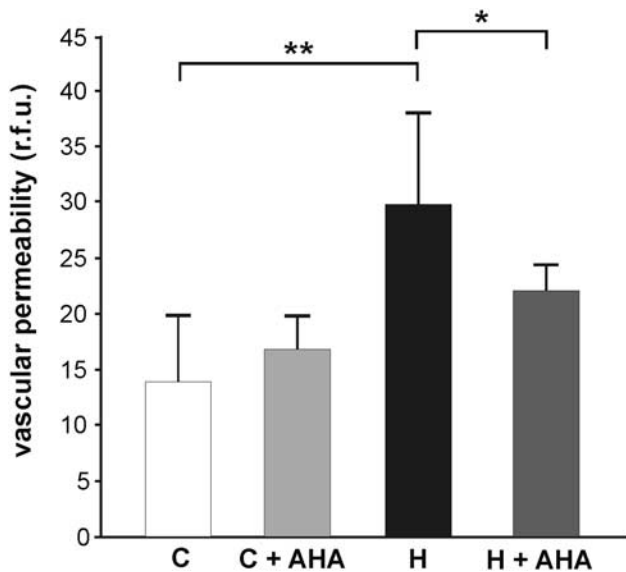
Figure 5 The MMP inhibition blunts vascular leakage *in vivo*. Mice received 60 mg/kg p-aminobenzoyl-gly-pro-D-leu-D-ala-hydroxamate (AHA) intraperitoneal (ip) (+ AHA) or vehicle as control and were exposed to 8% oxygen for 48 h (H) or kept at room air (C). Sodium fluorescein injection was used to quantify vascular permeability. After cardiac perfusion, fluorescence was quantified per mg of brain tissue (in relative fluorescence units, r.f.u.). The MMP inhibition significantly reduced hypoxia-induced hyperpermeability, but had no effect under normoxic conditions. Values are means ± s.d. (*$P < 0.05$, **$P < 0.001$; $n = 4$ to 5 animals per group).

hypoxia leads to MMP-9 activation specific in vascular structures, (3) inhibition of MMP activation attenuates vascular hyperpermeability and prevents gap formation and TJ rearrangement in cerebral endothelial cells, and (4) hypoxia-induced MMP-9 activation associated with vascular leakage depends on VEGF stimulation. To the best of our knowledge, this is the first *in vivo* examination of the BBB during normal flow and prolonged hypoxia without reoxygenation with assessment of vascular leakage, TJ protein rearrangement, and MMP activation. In contrast to cerebral ischemia, which is associated with severe BBB breakdown (as judged from albumin and Evans blue extravasation) and inflammation (Sandoval and Witt, 2008), our findings support the hypothesis that exposure to systemic hypoxia *per se* (without signs of inflammation and severe BBB breakdown) causes vascular leakage via VEGF-mediated activation of MMP-9 in cerebral micro-vasculature, leading to rearrangement and gap formation of the TJ proteins occludin and Zo-1. The hypoxia-induced vascular leakage is subtle, as the BBB becomes leaky only to the small tracer sodium fluorescein that does not cross an intact BBB (Schoch *et al*, 2002), but not to Evans blue or albumin (data not shown). The results further provide evidence for the therapeutic use of MMP inhibitors for treatment of cerebral edema caused by tissue hypoxia, as found in brain injury, ischemia, and high-altitude illness.

Hypoxia-Induced Hyperpermeability Correlates with Tight Junction Rearrangement

Hypoxia is a strong inducer of VEGF expression in the brain (Marti and Risau, 1998). The VEGF, a powerful angiogenic and neuroprotective factor (Zacchigna *et al*, 2008), but originally identified as vascular permeability factor in tumors, causes vascular leakage in the hypoxic and ischemic brain (Schoch *et al*, 2002; Wang *et al*, 2005). However, the underlying mechanisms *in vivo* are not well understood. Several *in vitro* studies suggested that hypoxia and/or VEGF interfere with TJ proteins, either on the level of expression, protein phosphorylation or cellular localization, while hardly any data on the effects of tissue hypoxia *in vivo* exist.

The results on the effect of hypoxia on expression level of TJ proteins are conflicting. *In vitro*, we previously showed a decrease of Zo-1 expression after hypoxia in cultured endothelial cells (Fischer *et al*, 2002, 2004), but others observed no significant changes in protein expression of either occludin or Zo-1 in bovine BMECs under the same conditions (Brown *et al*, 2003; Mark and Davis, 2002) or at 6 h exposure to hypoxia (Brown and Davis, 2005). However, on posthypoxic reoxygenation, both Zo-1 and occludin expression was significantly elevated (Mark and Davis, 2002). Furthermore, hypoxia was associated with reduced claudin-5 expression *in vitro* (Koto *et al*, 2007). We found a diminished occludin expression, but no change in either Zo-1 or claudin-5 in our *in vivo* model of prolonged (48 h) tissue hypoxia. The differences might depend on the *in vivo* situation or the lack of a reoxygenation period in our model. Hardly any other studies addressing direct effects of prolonged tissue hypoxia exist. In one study, rats were exposed to 6% oxygen, but only for 1 h followed by 10 mins reoxygenation. Under these conditions, no significant difference in Zo-1 or occludin expression compared with controls were found, except that phosphorlyation of occludin was changed after reoxygenation (Witt *et al*, 2003). However, using the same hypoxia/reoxygenation model, a recent study showed alteration of occludin oligomeric assembly at TJ (McCaffrey *et al*, 2009), suggesting in accordance with our findings, that occludin is the principal TJ component influenced by hypoxia.

Thus, although the effects of hypoxia on TJ protein expression seem to be context dependent, our *in vivo* results of TJ rearrangement of occludin and Zo-1, and gap formation as a consequence of tissue hypoxia are in line with earlier *in vitro* findings. We previously showed a correlation of hypoxia-induced and VEGF-mediated hyperpermeability with disruption of Zo-1 staining in BMECs in culture (Fischer *et al*, 2000, 2002, 2004). Another study also showed that hypoxia disrupted the continuous pericellular distribution of occludin and Zo-1 *in vitro* (Mark and Davis, 2002). Others have also reported a disruption in claudin-5 expression after hypoxic exposure (Koto *et al*, 2007).
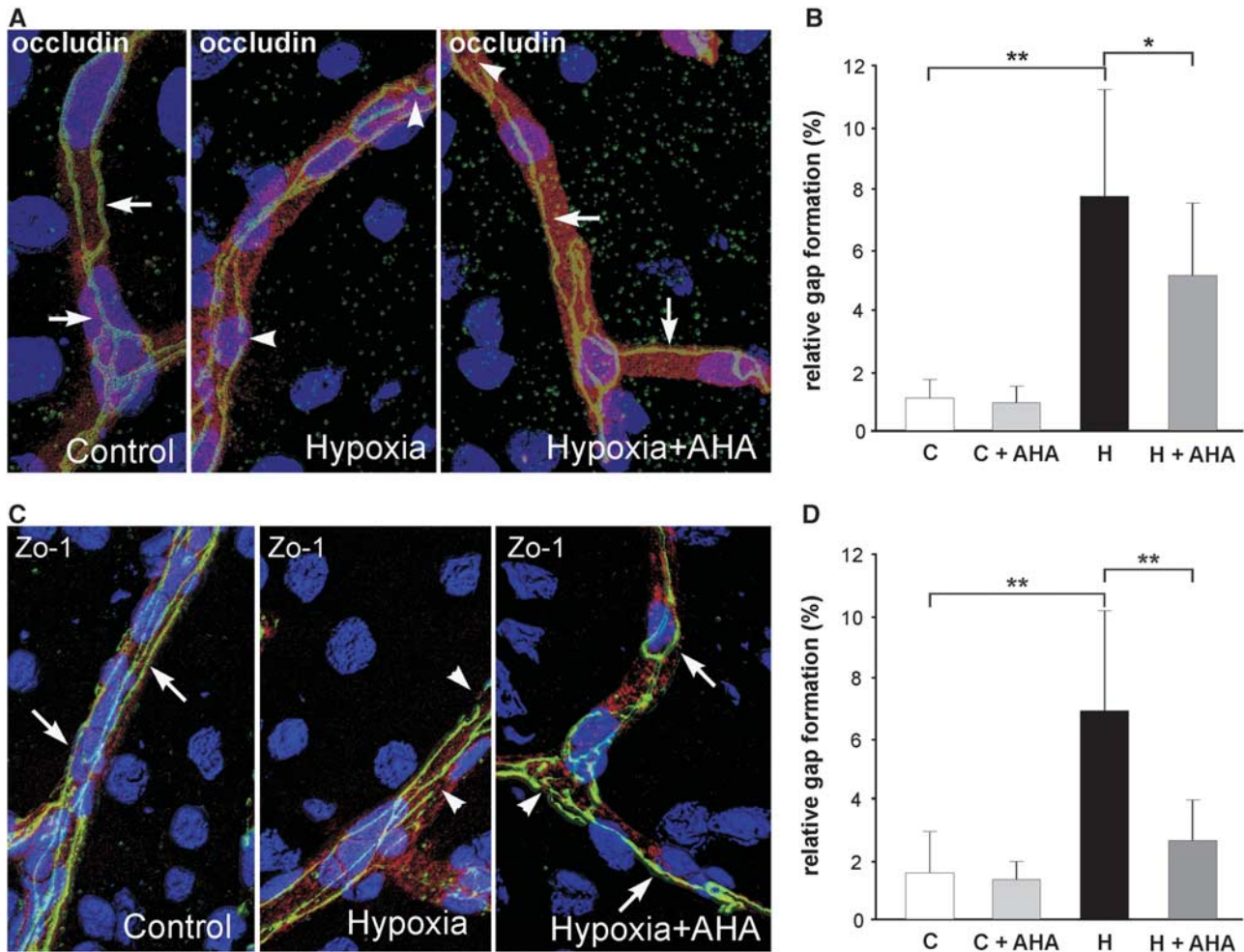
Figure 6 The MMP inhibition reverts rearrangement and gap formation of occludin and Zo-1. After pretreatment with p-aminobenzoyl-gly-pro-D-leu-D-ala-hydroxamate (+ AHA) or vehicle mice were exposed to hypoxia for 48 h at 8% oxygen (H) or kept at room air (C). Thereafter, cryosections from cortex were stained for occludin and Zo-1, and co-stained with platelet endothelial cell adhesion molecule-1 (Pecam-1). Nuclei were stained with 4,6-diamidino-2-phenylindole (DAPI). (**A**, **C**) Three-dimensional reconstruction after confocal microscopy depicting continuous, linear, and sharp labeling of occludin and Zo-1 along the whole vessel (arrows), and discontinuous, irregular and diffuse staining and gap formation (arrowheads). (**A**, **B**) Pretreatment with AHA significantly reduced hypoxia-induced redistribution and relative gap formation by 30% for occludin, and (**D**) by 60% for Zo-1. Values are means ± s.d. (*$P < 0.05$, **$P < 0.001$; $n = 3$ to 5 animals per group).

However, we found no effect of hypoxia on claudin-5 localization. Taken together, our data indicate that vascular leakage *in vivo* after prolonged exposure to hypoxia directly correlates with gap formation and rearrangement of the TJ proteins occludin and Zo-1.

Hypoxia-Induced Vascular Leakage and Tight Junction Rearrangement is Mediated by Matrix Metalloproteinase-9

Although specific mediators in the regulation of TJ have been identified, the exact mechanisms of how TJ are directly affected by hypoxia remain to be determined. Our results strongly indicate a direct function of MMPs for vascular leakage and TJ rearrangement as (1) hypoxia resulted in a vascular-specific increase of MMP activity, (2) treatment with

an MMP inhibitor significantly attenuated vascular leakage after hypoxic exposure, and (3) MMP inhibition prevented TJ rearrangement and gap formation.

Earlier studies have mainly addressed the role of MMPs in cerebral ischemia. However, as inflammatory processes are of major importance during cerebral ischemia, and it is well known that MMPs are activated during inflammation, our results are not directly comparable, as in our tissue hypoxia model, no signs of inflammation are present. Nevertheless, our findings are in line with earlier ischemia studies, showing that MMP inhibition reduced BBB damage (Gasche *et al*, 2001) and attenuated disruption of TJ (Yang *et al*, 2007).

In the adult brain, MMP expression levels are very low or undetectable, but many MMPs are upregulated in neurons, astrocytes, oligodendrocytes, microglia, and endothelial cells after injury

846
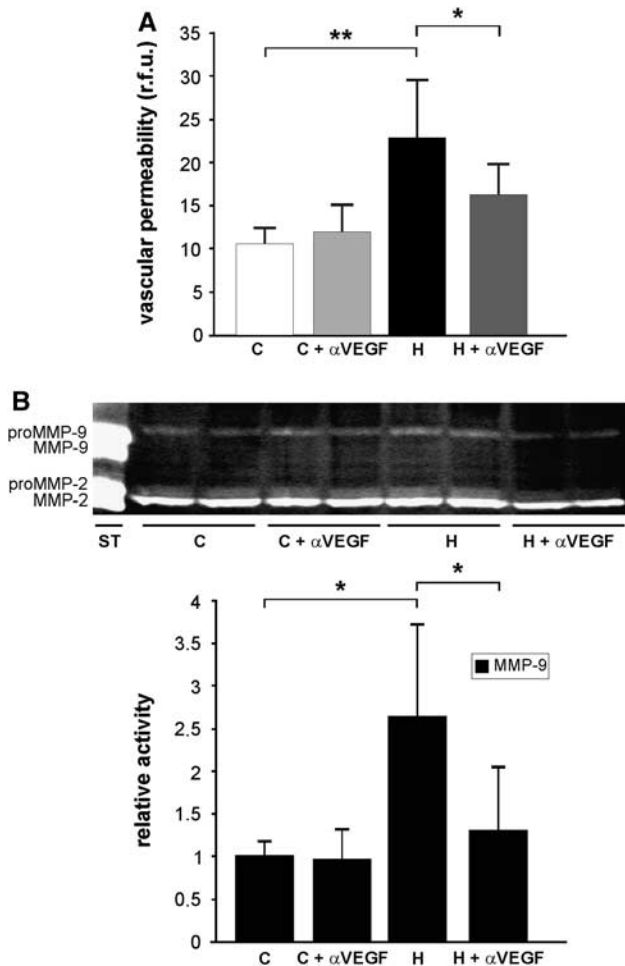
Figure 7 The VEGF inhibition reduces hypoxia-induced MMP-9 activity. (**A**) Mice receiving ip 10 mg/kg bevacizumab (Avastin) (+ αVEGF) or vehicle were exposed to 8% oxygen for 48 h (H) or kept at room air (C). Sodium fluorescein was used to quantify vascular permeability. Fluorescence was quantified per mg of brain tissue (in relative fluorescence units, r.f.u.). The VEGF inhibition significantly attenuated hypoxia-induced vascular permeability, but had no effect under normoxic conditions. Values are means ± s.d. (*$P < 0.05$, **$P < 0.001$; $n = 6$ animals per group). (**B**) Representative gelatin zymography demonstrating MMP-9 upregulation after of hypoxia (H) compared with normoxic control (C). Treatment with bevacizumab significantly attenuated MMP-9 upregulation in hypoxic brains. Bars show mean values (± s.d.) of relative gelatinolytic activity (*$P < 0.05$; $n = 3$ to 6 animals per group).

(Cunningham et al, 2005). Unfortunately, a direct identification of MMP-2 and -9 by immunofluorescence in situ was not feasible, as appropriate antibodies were not available. A combination of in situ with gel zymography allowed us to identify the specific gelatinolytic activity in microvascular structures during hypoxia to be MMP-9 as the relevant proteinase involved in hypoxic BBB degradation. Both MMP-2 and MMP-9 had been suggested to be involved in cerebral BBB breakdown (Lee et al, 2007; Yang et al, 2007). Our gel zymography experiments indicate MMP-9 as the relevant enzyme, due to

a higher activity of both the latent proform and the active enzyme, whereas MMP-2 was unchanged after hypoxia. Furthermore, the inhibitor leading to decreased vascular permeability strongly inhibited MMP-9, but not MMP-2. Further evidence for the involvement of MMP-9, but not MMP-2 comes from various knock-out models. Although MMP-9-deficient mice showed reduced BBB damage after focal cerebral ischemia (Asahi et al, 2001b), no effect was seen in MMP-2-deficient mice after stroke (Asahi et al, 2001a). Furthermore, the type of MMP involved in BBB breakdown might depend on the duration of hypoxic exposure. Indeed, although elevated MMP-2 activity correlated with initiation of ischemia (Chang et al, 2003) and early BBB opening (Yang et al, 2007), MMP-9 activity was associated with delayed phases of BBB disruption and vasogenic edema formation (Lee et al, 2007). Accordingly, our results using prolonged hypoxia without inflammatory response identify MMP-9 as the major player resulting in vascular leakage.

Mechanism of Matrix Metalloproteinase Action on Tight Junction Rearrangement

It remains to be established how MMP activation results in TJ rearrangement. Earlier investigations in ischemia have focused on the cerebrovascular basal lamina. As both collagen IV and laminin are MMP-9 substrates, it was speculated that proteolysis of these components would perturb BBB integrity leading to vasogenic edema (Hamann et al, 1995). However, MMPs could directly interact with TJ proteins resulting in their degradation and thus reduced protein expression levels. Indeed, we observed a loss of occludin expression after hypoxia, indicative of occludin degradation. In retinal endothelial and pigment epithelial cells, MMP treatment was correlated with proteolytic degradation of occludin, whereas no effect on claudin-5 was noted (Giebel et al, 2005). These findings are in line with our results that occludin, but not claudin-5 is the relevant target for hypoxia-induced TJ integrity loss. Further evidence for a direct action of MMPs on TJ proteins comes from MMP-9-deficient mice that showed reduced Zo-1 degradation following ischemia as compared with control (Asahi et al, 2001b). Furthermore, increased MMP-2 and MMP-9 levels resulted in the degradation of occludin after focal ischemia/reperfusion, which was reversed by MMP inhibition (Yang et al, 2007). Direct evidence comes from experiments showing that occludin contains a putative extracellular MMP cleavage site (Bojarski et al, 2004) and is a direct substrate for MMPs (Wachtel et al, 1999). Very recently, it was shown in focal cerebral ischemia that normobaric hyperoxia attenuates BBB disruption by inhibiting MMP-9-mediated occludin degradation (Liu et al, 2009), again supporting our findings, that hypoxia results in vascular leakage by activation of MMP-9 with subsequent occludin degradation.

Role of Vascular Endothelial Growth Factor for Matrix Metalloproteinase-9 Activation and Tight Junction Rearrangement

There is good evidence that the effects of tissue hypoxia on vascular leakage are mediated through VEGF. First, VEGF is induced by systemic hypoxia in the brain (Marti and Risau, 1998), and hypoxia-induced vascular leakage is blocked by neutralizing VEGF antibodies (Schoch et al, 2002). Second, VEGF can mediate changes of TJ protein expression and rearrangement (Fischer et al, 2002; Wang et al, 2001; Yeh et al, 2007). Third, a direct activation of MMP-9 by VEGF has been shown (Hollborn et al, 2007; Valable et al, 2005). Our results (Figure 7) strengthen the idea that VEGF increases vascular leakage via MMP-9 activation, as blocking VEGF action using bevacizumab (Avastin) not only reduced vascular leakage but also attenuated hypoxic MMP-9 activity. It remains to be established how VEGF affects TJ rearrangement. One possibility is that VEGF regulates vascular permeability via phosphorylation of TJ proteins (Antonetti et al, 1999).

On the basis of these results, an anti-VEGF strategy to treat brain edema seems promising; however, as VEGF is also a potent neuroprotective factor (Greenberg and Jin, 2005), might have adverse side effects. Interfering with specific downstream signaling pathways of VEGF might be an alternative. Hypoxia-induced vascular leakage in vivo can be blocked by inhibition of p38 (Issbrücker et al, 2003), and PI3K/Akt pathways (Vogel et al, 2007). However, as the same pathways also mediate the neuroprotective effect of VEGF (Greenberg and Jin, 2005), this may not be helpful either. Thus, blocking further downstream signals such as MMP-9 for treatment of hypoxia-induced edema might be a better target, as has been suggested for ischemic brain injuries (Gasche et al, 2001).

In summary, we have shown that vascular leakage in the brain in vivo, induced by normobaric hypoxia, is mediated by MMP-9-dependent TJ rearrangement. The mechanistic insights into the pathophysiologic changes associated with tissue hypoxia and the cerebral microvasculature in vivo provide the basis for therapeutic strategies to treat brain edema based on inhibition of MMP activity.

Disclosure/conflict of interest

The authors declare no conflict of interest.

References

Antonetti DA, Barber AJ, Hollinger LA, Wolpert EB, Gardner TW (1999) Vascular endothelial growth factor induces rapid phosphorylation of tight junction proteins occludin and zonula occludens 1. A potential mechanism for vascular permeability in diabetic retinopathy and tumors. J Biol Chem 274:23463–7

Asahi M, Sumii T, Fini ME, Itohara S, Lo EH (2001a) Matrix metalloproteinase 2 gene knockout has no effect on acute brain injury after focal ischemia. Neuroreport 12:3003–7

Asahi M, Wang X, Mori T, Sumii T, Jung JC, Moskowitz MA, Fini ME, Lo EH (2001b) Effects of matrix metalloproteinase-9 gene knock-out on the proteolysis of blood-brain barrier and white matter components after cerebral ischemia. J Neurosci 21:7724–32

Bojarski C, Weiske J, Schöneberg T, Schröder W, Mankertz J, Schulzke J, Florian P, Fromm M, Tauber R, Huber O (2004) The specific fates of tight junction proteins in apoptotic epithelial cells. J Cell Sci 117:2097–107

Brown RC, Davis TP (2005) Hypoxia/aglycemia alters expression of occludin and actin in brain endothelial cells. Biochem Biophys Res Commun 327:1114–23

Brown RC, Mark KS, Egleton RD, Huber JD, Burroughs AR, Davis TP (2003) Protection against hypoxia-induced increase in blood-brain barrier permeability: role of tight junction proteins and NFkappaB. J Cell Sci 116:693–700

Chang D, Hosomi N, Lucero J, Heo J, Abumiya T, Mazar AP, del Zoppo GJ (2003) Activation systems for latent matrix metalloproteinase-2 are upregulated immediately after focal cerebral ischemia. J Cereb Blood Flow Metab 23:1408–19

Cunningham LA, Wetzel M, Rosenberg GA (2005) Multiple roles for MMPs and TIMPs in cerebral ischemia. Glia 50:329–39

Fischer S, Wiesnet M, Marti HH, Renz D, Schaper W (2004) Simultaneous activation of several second messengers in hypoxia-induced hyperpermeability of brain derived endothelial cells. J Cell Physiol 198:359–69

Fischer S, Wobben M, Kleinstück J, Renz D, Schaper W (2000) Effect of astroglial cells on hypoxia-induced permeability in PBMEC cells. Am J Physiol Cell Physiol 279:C935–44

Fischer S, Wobben M, Marti HH, Renz D, Schaper W (2002) Hypoxia-induced hyperpermeability in brain microvessel endothelial cells involves VEGF-mediated changes in the expression of zonula occludens-1. Microvasc Res 63:70–80

Gasche Y, Copin JC, Sugawara T, Fujimura M, Chan PH (2001) Matrix metalloproteinase inhibition prevents oxidative stress-associated blood-brain barrier disruption after transient focal cerebral ischemia. J Cereb Blood Flow Metab 21:1393–400

Giebel SJ, Menicucci G, McGuire PG, Das A (2005) Matrix metalloproteinases in early diabetic retinopathy and their role in alteration of the blood-retinal barrier. Lab Invest 85:597–607

Greenberg DA, Jin K (2005) From angiogenesis to neuropathology. Nature 438:954–9

848

Hackett PH, Roach RC (2001) High-altitude illness. *N Engl J Med* 345:107–14

Hamann GF, Okada Y, Fitridge R, del Zoppo GJ (1995) Microvascular basal lamina antigens disappear during cerebral ischemia and reperfusion. *Stroke* 26:2120–6

Hawkins BT, Davis TP (2005) The blood-brain barrier/neurovascular unit in health and disease. *Pharmacol Rev* 57:173–85

Hollborn M, Stathopoulos C, Steffen A, Wiedemann P, Kohen L, Bringmann A (2007) Positive feedback regulation between MMP-9 and VEGF in human RPE cells. *Invest Ophthalmol Vis Sci* 48:4360–7

Issbrücker K, Marti HH, Hippenstiel S, Springmann G, Voswinckel R, Gaumann A, Breier G, Drexler HCA, Suttorp N, Clauss M (2003) p38 MAP kinase—a molecular switch between VEGF-induced angiogenesis and vascular hyperpermeability. *FASEB J* 17:262–4

Kallenberg K, Bailey DM, Christ S, Mohr A, Roukens R, Menold E, Steiner T, Bärtsch P, Knauth M (2007) Magnetic resonance imaging evidence of cytotoxic cerebral edema in acute mountain sickness. *J Cereb Blood Flow Metab* 27:1064–71

Kilic E, Kilic U, Wang Y, Bassetti CL, Marti HH, Hermann DM (2006) The phosphatidylinositol-3 kinase/Akt pathway mediates VEGF's neuroprotective activity and induces blood brain barrier permeability after focal cerebral ischemia. *FASEB J* 20:1185–7

Kleiner DE, Stetler-Stevenson WG (1994) Quantitative zymography: detection of picogram quantities of gelatinases. *Anal Biochem* 218:325–9

Koto T, Takubo K, Ishida S, Shinoda H, Inoue M, Tsubota K, Okada Y, Ikeda E (2007) Hypoxia disrupts the barrier function of neural blood vessels through changes in the expression of claudin-5 in endothelial cells. *Am J Pathol* 170:1389–97

Lee CZ, Xue Z, Zhu Y, Yang G, Young WL (2007) Matrix metalloproteinase-9 inhibition attenuates vascular endothelial growth factor-induced intracerebral hemorrhage. *Stroke* 38:2563–8

Liu W, Hendren J, Qin X, Shen J, Liu KJ (2009) Normobaric hyperoxia attenuates early blood-brain barrier disruption by inhibiting MMP-9-mediated occludin degradation in focal cerebral ischemia. *J Neurochem* 108:811–20

Mark KS, Davis TP (2002) Cerebral microvascular changes in permeability and tight junctions induced by hypoxia-reoxygenation. *Am J Physiol Heart Circ Physiol* 282:H1485–94

Marti HH, Risau W (1998) Systemic hypoxia changes the organ-specific distribution of vascular endothelial growth factor and its receptors. *Proc Natl Acad Sci USA* 95:15809–14

McCaffrey G, Willis CL, Staatz WD, Nametz N, Quigley CA, Hom S, Lochhead JJ, Davis TP (2009) Occludin oligomeric assemblies at tight junctions of the blood-brain barrier are altered by hypoxia and reoxygenation stress. *J Neurochem* 110:58–71

Rosenberg GA (2009) Matrix metalloproteinases and their multiple roles in neurodegenerative diseases. *Lancet Neurol* 8:205–16

Sandoval KE, Witt KA (2008) Blood-brain barrier tight junction permeability and ischemic stroke. *Neurobiol Dis* 32:200–19

Schoch HJ, Fischer S, Marti HH (2002) Hypoxia-induced vascular endothelial growth factor expression causes vascular leakage in the brain. *Brain* 125:2549–57

Valable S, Montaner J, Bellail A, Berezowski V, Brillault J, Cecchelli R, Divoux D, Mackenzie ET, Bernaudin M, Roussel S, Petit E (2005) VEGF-induced BBB permeability is associated with an MMP-9 activity increase in cerebral ischemia: both effects decreased by Ang-1. *J Cereb Blood Flow Metab* 25:1491–504

Vogel C, Bauer A, Wiesnet M, Preissner KT, Schaper W, Marti HH, Fischer S (2007) Flt-1, but not Flk-1 mediates hyperpermeability through activation of the PI3-K/Akt pathway. *J Cell Physiol* 212:236–43

Wachtel M, Frei K, Ehler E, Fontana A, Winterhalter K, Gloor SM (1999) Occludin proteolysis and increased permeability in endothelial cells through tyrosine phosphatase inhibition. *J Cell Sci* 112(Pt 23):4347–56

Wang W, Dentler WL, Borchardt RT (2001) VEGF increases BMEC monolayer permeability by affecting occludin expression and tight junction assembly. *Am J Physiol Heart Circ Physiol* 280:H434–40

Wang Y, Kilic E, Kilic U, Weber B, Bassetti CL, Marti HH, Hermann DM (2005) VEGF overexpression induces post-ischaemic neuroprotection, but facilitates haemodynamic steal phenomena. *Brain* 128:52–63

Witt KA, Mark KS, Hom S, Davis TP (2003) Effects of hypoxia-reoxygenation on rat blood-brain barrier permeability and tight junctional protein expression. *Am J Physiol Heart Circ Physiol* 285:H2820–31

Yang Y, Estrada EY, Thompson JF, Liu W, Rosenberg GA (2007) Matrix metalloproteinase-mediated disruption of tight junction proteins in cerebral vessels is reversed by synthetic matrix metalloproteinase inhibitor in focal ischemia in rat. *J Cereb Blood Flow Metab* 27:697–709

Yeh W, Lu D, Lin C, Liou H, Fu W (2007) Inhibition of hypoxia-induced increase of blood-brain barrier permeability by YC-1 through the antagonism of HIF-1alpha accumulation and VEGF expression. *Mol Pharmacol* 72:440–9

Zacchigna S, Lambrechts D, Carmeliet P (2008) Neurovascular signalling defects in neurodegeneration. *Nat Rev Neurosci* 9:169–81